A Novel Filtering Method to Extract Three Critical Yield Loss Components (Gross, Repeated, and Random) FIMER

Kiyotaka Imai, *Member, IEEE,* and Toru Kaga, *Member, IEEE*

***Abstract*—This paper describes a novel filtering method (FIMER) to extract three critical yield loss components: gross yield loss from parametric problems or from clustering of defects, repeated yield loss from mask defects or from lithography margin, and random yield loss mainly from particles. It is shown by simulation that FIMER is not only superior to the conventional windowing method in extracting repeated yield loss but also accurately extracts gross yield loss and random yield loss. The simulation studies show that the three components are extracted with an error equal to or less than 5% by optimizing threshold and filter weights, which are the major parameters in FIMER.**

***Index Terms*—Filter, simulation, yield improvement, yield loss.**

I. Introduction

TO IDENTIFY process-related problems, it is very effective to extract yield loss components and analyze their spatial patterns [1]. For example, plasma processing is often the cause of center loss, or mask defects generate a checkerboard pattern on the entire wafer. However, it is not rare to miss these specific patterns because a probe-tested wafer map is a mixture of various kinds of yield loss components.

Yield loss has three critical components: gross yield loss from parametric problems or from clustering of defects, repeated yield loss from mask defects or from lithography margin, and random yield loss mainly from particles.

Among the yield models proposed in the past [1]–[6], the yield models [1], [2] add a constant multiplier C to a simple Poisson model or Murphy model to account for a large-area yield loss, called gross yield loss in this paper. With these models, the windowing method [3] has been successfully used to extract gross yield loss and random yield loss and has contributed to improving yield especially from a parametric point of view [7], [8].

On the contrary, although repeated yield loss also becomes crucial as the lithography process becomes more and more important with shrinkage of device size [9], it has not often been discussed within the context of the windowing method.

Recently, it has been shown that the windowing method has difficulty in extracting repeated yield loss because repeated yield loss largely contributes to random yield loss in the windowing method. A new method called FIMER has been proposed [10]. It is also shown that FIMER is effective not only for repeated yield loss but also for gross yield loss and for random yield loss [11].

In addition to extracting the three components as quantity, FIMER also shows both gross yield loss and repeated yield loss on a wafer map, although mapping of gross yield loss is reported [12]. These features of FIMER help to identify process-related problems. Correlation between gross yield loss and parametric values will identify significant parameters affecting yield. If repeated yield loss is compared between lithography tools, tools with lithography problems would be listed. To evaluate the impact of random defects on yield, the wafer regions with gross and repeated yield loss are excluded.

In this paper, the yield model in FIMER is compared with that in the windowing method in Section II. The procedure to extract three yield loss components (gross, repeated, random) in FIMER is shown in Section III. In Section IV, simulated results will be discussed in relation to threshold and filter weights, which are the major parameters in FIMER [13]. Here, the simulation studies show that the three components are extracted with an error equal to or less than 5% when threshold and filter weights are optimized. After briefly discussing the application of FIMER to a product wafer in Section V, this paper is concluded in Section VI.

II. Yield Model in FIMER

In the windowing method, probe yield Y is given by [8]

$$Y = YsYr \tag{1}$$

$$Yr = \exp(-AD) \tag{2}$$

where

- Ys and Yr yield components limited by systematic yield loss (constant multiplier C in Section I) and by random yield loss, respectively;
- A active area of a die;
- D average defect density; Poisson distribution is assumed for random defects.

Here, systematic yield loss refers to nonrandom spatial distribution and random yield loss refers to random spatial distribution of failed dies, respectively.

The way to extract Ys and Yr in the windowing method is as follows. By grouping neighboring dies, a multiple die larger than the original die with size A is formed. Here, the multiple

Manuscript received July 14, 2000.

The authors are with the Yield Management Consulting Group, KLA-Tencor Japan Ltd., Kanagawa 240-0005, Japan (e-mail: kiyotaka.imai@kla-tencor.com; toru.kaga@kla-tencor.com).

Publisher Item Identifier S 0894-6507(00)09489-6.

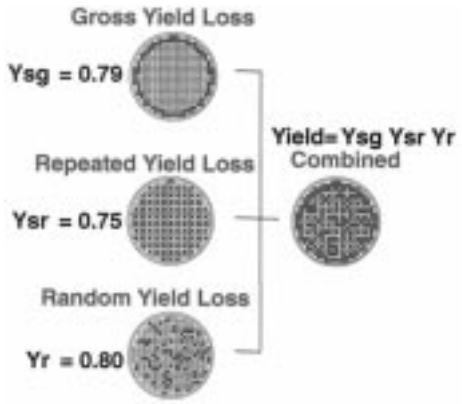

Fig. 1. An example of a combined wafer map: dark marks are failed dies.

die is defined as a good die only if all of its components are good dies. This is how the yield of a multiple die is derived. Once the yield for a multiple die with different size is derived, Ys and Yr are extracted by (1) and (2).

The windowing method has been effectively used for parametric analysis [8] because parametric problems often cause gross yield loss and Ys in (1) has its origin as a multiplier to account for gross yield loss [1]. On the contrary, although repeated yield loss is also systematic yield loss, it has not often been discussed whether the windowing method extracts repeated yield loss as systematic yield loss. Recently, it has been shown by simulation that a large portion of repeated yield loss is extracted as random yield loss, not as systematic yield loss [10].

Therefore, a new method to separate repeated yield loss from random yield loss is needed. In FIMER, to account for gross yield loss as well as repeated yield loss, probe yield Y is given by [11]

$$Y = YsgYsrYr \tag{3}$$

where Ysg, Ysr, and Yr are the yield components limited by gross yield loss, by repeated yield loss, and by random yield loss, respectively. As known from (3), in FIMER, it is not necessary to assume a particular distribution for random defects as done in the windowing method. Using spatial information on a binary wafer map (1 for Pass and 0 for Fail), FIMER extracts the three yield loss components by a new filtering technique described in the following section.

In the simulation studies, an artificially generated combined map shown in Fig. 1 is used as input for FIMER. Here, the combined map is a binary map in which 1 is assigned for Pass and 0 for Fail. Using the combined map, three yield components are extracted (ysg, ysr, yr) by FIMER, and the extracted components are compared to the original ones (Ysg, Ysr, Yr) to evaluate how accurately FIMER extracts the three yield loss components. The original yield components, Ysg, Ysr, and Yr, are given by

$$Ysg = (N - Nsg)/N \tag{4}$$
$$Ysr = (N - Nsg - Nsr)/(N - Nsg) \tag{5}$$
$$Yr = (Y/Ysg)/Ysr \tag{6}$$

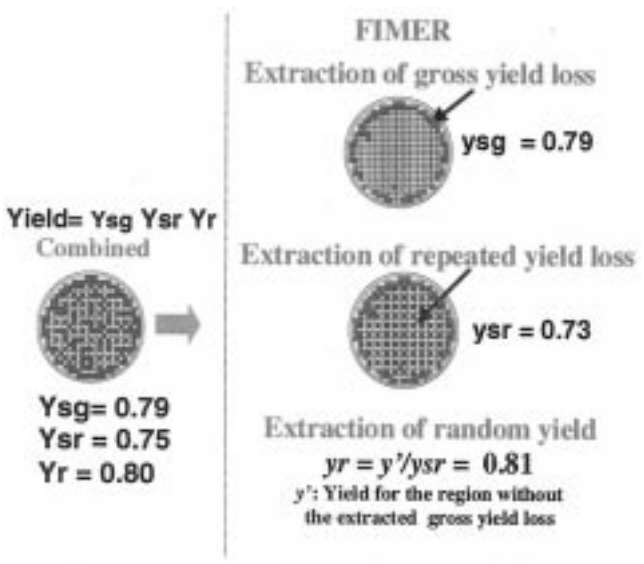

Fig. 2. An example of FIMER: edge loss as gross yield loss.

where

- N total number of dies on a combined wafer;
- Nsg number of dies in the gross yield loss on a combined map;
- Nsr number of dies in the repeated yield loss on a combined map.

In the windowing method, two yield loss components (gross and random) are extracted only as quantity (compliment of yield component Ys, Yr). In FIMER, not only are three yield loss components (gross, repeated, and random) extracted as quantity but also gross yield loss and repeated yield loss are shown on a wafer map, as in Fig. 2.

III. Extracting Procedure by FIMER

First is the extraction of ysg, which is given by

$$ysg = (N - nsg)/N \tag{7}$$

where nsg is the number of extracted dies as gross yield loss.

The procedure to extract nsg is shown in Fig. 3. By smoothing, a combined map with binary data (1 for Pass, 0 for Fail) is converted to an analog map where each die has a value between zero and one. The 3×3 die filter shown in Fig. 3 is basically the same as that used in image processing [14] if each die is considered as a pixel. Then, by setting an optimum threshold for the analog map [15], a new binary map that only shows the extracted dies as gross yield loss is derived. The operation of smoothing and thresholding is defined as filtering in this paper.

The effect of smoothing is graphically shown in Fig. 4. Before smoothing, it is not possible to separate gross yield loss from others because the dies in the gross yield loss have the same value (0) with other failed dies, as shown in Fig. 4(a). However, by smoothing, the distribution of analog data for the gross yield loss is separated from that of others. Therefore, by setting an optimal threshold, most of the dies in the gross yield loss on

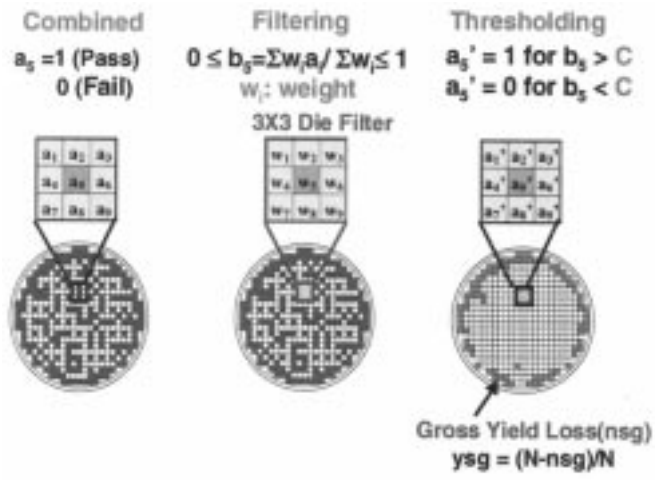

Fig. 3. Extraction of gross yield loss by FIMER: N is the total number of dies on a wafer; nsg is the number of extracted dies as gross yield loss.

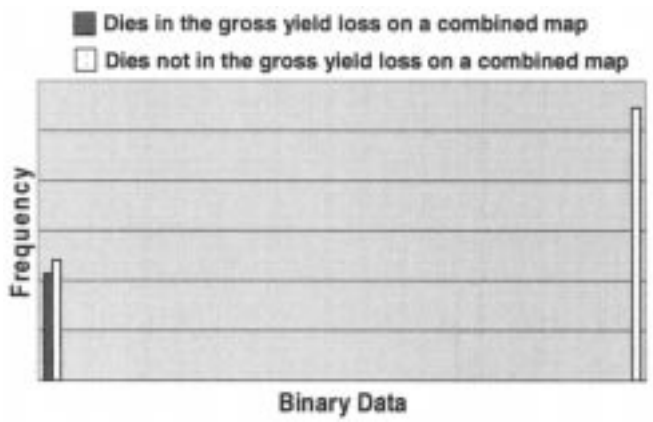

(a)

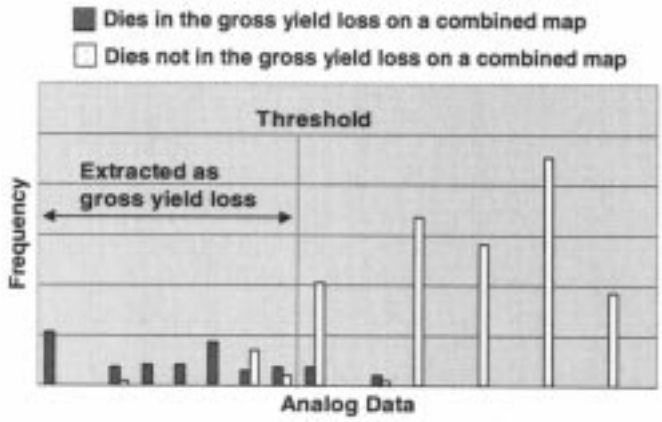

(b)

Fig. 4. (a) Distributions of binary data for a combined map (binary map): it is not possible to separate the dies in the gross yield loss on a combined map from others by thresholding. (b) Distributions of analog data for an analog map after smoothing: by setting an optimal threshold, most of the dies in the gross yield loss on a combined map are extracted as gross yield loss for a new binary map.

a combined map are extracted as gross yield loss, as shown in Fig. 4(b). In Fig. 4(b), the overlap between two distributions is one of the major causes of error in extraction. Optimization for filter weights minimizes the overlap and will be discussed in Section IV.

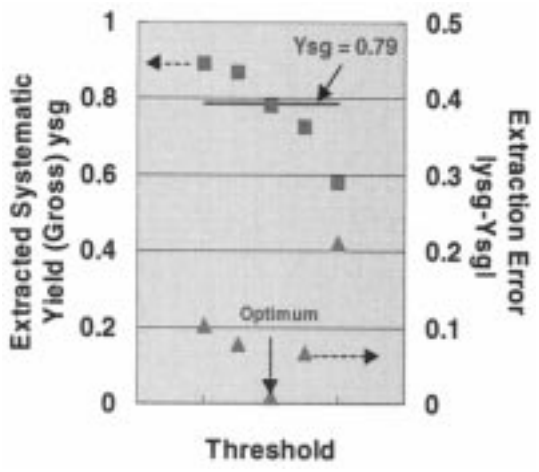

Fig. 5. Effect of threshold on extraction error of ysg ($|ysg - Ysg|$). An optimal threshold is defined as the threshold that minimizes the extraction error $|ysg - Ysg|$.

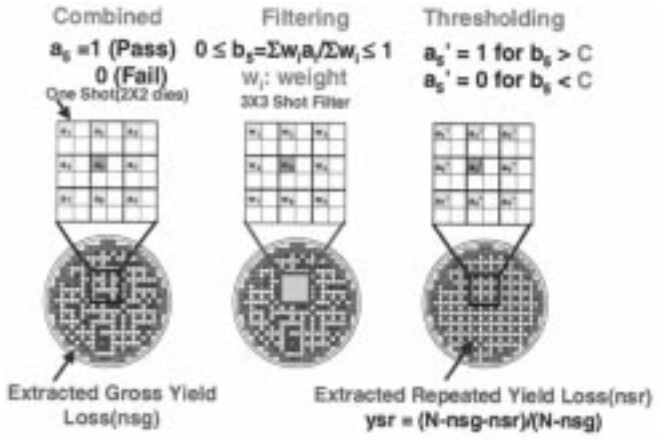

Fig. 6. Extraction of repeated yield loss by FIMER: N is the total number of dies on a wafer, nsg is the number of extracted dies as gross yield loss, and nsr is the number of extracted dies as repeated yield loss.

In the simulation studies, an optimal threshold is defined as the threshold that minimizes the extraction error of ysg ($|ysg - Ysg|$). This is graphically shown in Fig. 5, in which an optimal threshold (optimum in Fig. 5) minimizes the extraction error $|ysg - Ysg|$.

Next is the extraction of ysr, which is given by

$$ysr = (N - nsg - nsr)/(N - nsg) \tag{8}$$

where nsr is the number of extracted dies as repeated yield loss. As shown in Fig. 6, nsr is extracted by filtering, as in the case of gross yield loss (nsg). However, the filter is a 3×3 shot filter, where the dies belonging to the same field (top left field in Fig. 6) in the neighboring shots are used for filtering. Here, the dies extracted as gross yield loss are excluded from filtering. The concept is to extract the spatial frequency specific to the shot.

As in the case of the extraction of gross yield loss, threshold is adjusted to minimize the extraction error of ysr. Also, filtering weights have to be optimized to give better separation between repeated yield loss and others of an analog map derived by smoothing.

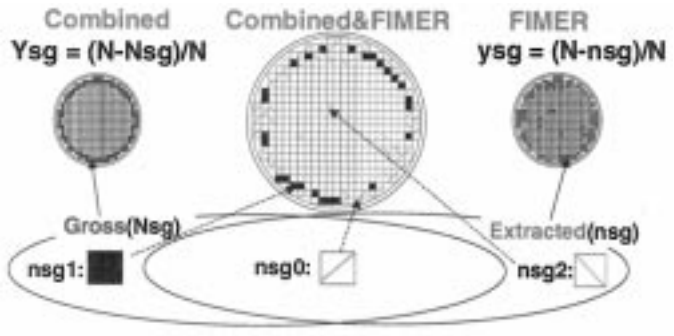

Fig. 7. The case where the extracted gross yield loss is not similar to that on a combined map even if $ysg \sim Ysg$.

Finally, yr is given by

$$yr = y'/ysr \tag{9}$$

where y' is the yield for the wafer region without the extracted gross yield loss.

IV. Simulated Results and Discussions

A. A New Measure for Parameter Optimization: Match Ratio

In FIMER, there are two parameters to consider: threshold and a set of filter weights, as seen in Figs. 3 and 6. Threshold is adjusted to minimize the extraction error of yield components (ysg, ysr), as shown in Fig. 5. However, there is a case where an extracted map is not what is expected from a combined map even if $ysg \approx Ysg$ (or $ysr \approx Ysr$). Fig. 7 shows this situation for gross yield loss, in which

$$Nsg = nsg0 + nsg1 \tag{10}$$

$$nsg = nsg0 + nsg2 \tag{11}$$

where

- $nsg0$ number of dies in the gross yield loss both on a combined map and on a map by FIMER;
- $nsg1$ number of dies in the gross yield loss only on a combined map;
- $nsg2$ number of dies in the gross yield loss only on a map by FIMER.

By setting an optimal threshold, it is possible to make $ysg \approx Ysg (nsg \approx Nsg)$. However, in the case $nsg1 > 0$ and/or $nsg2 > 0$, the extracted map deviates from what is expected from a combined map. The source of $nsg1$ and $nsg2$ is the overlap of two distributions in the histogram shown in Fig. 8. Filter weights have to be adjusted to minimize the overlap. Thus, as a new measure of optimization for filter weights, match ratio is introduced. In the extraction of gross yield loss, this is called gross match ratio Mg and is given by

$$Mg = nsg0/(nsg0 + nsg1 + nsg2). \tag{12}$$

As known from (12), optimization for filter weights maximizes Mg.

Similar to gross match ratio, match ratio for repeated yield loss Mrp is defined as follows:

$$Mrp = nsr0/(nsr0 + nsr1 + nsr2) \tag{13}$$

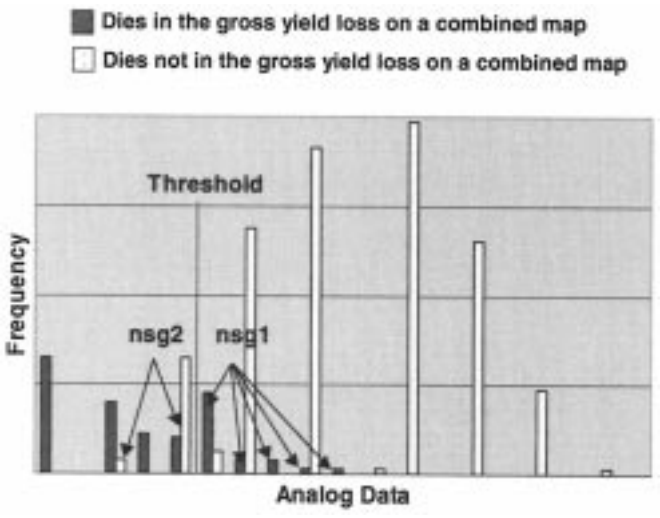

Fig. 8. Distributions of analog data for an analog map after smoothing for the combined map in Fig. 7. The more the overlap, the more the extracted gross yield loss deviates from that on a combined map.

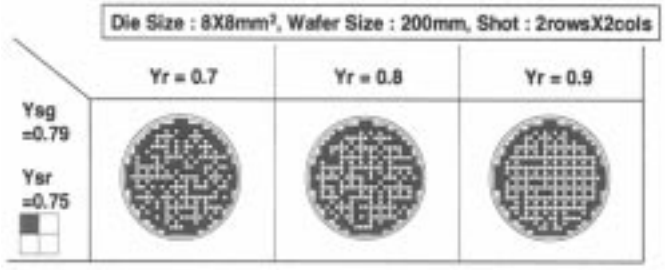

Fig. 9. Examples of simulated cases with $Ysg = 0.79$ (edge loss), $Ysr = 0.75$, and $Yr = 0.7, 0.8, 0.9$.

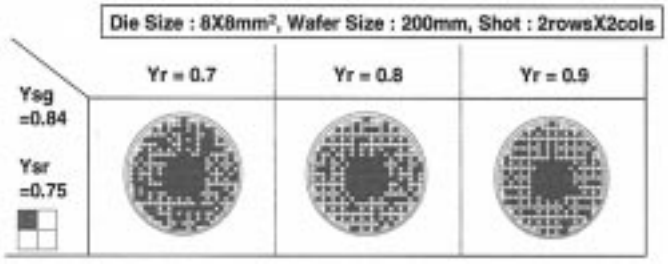

Fig. 10. Examples of simulated cases with $Ysg = 0.84$ (center loss), $Ysr = 0.75$, and $Yr = 0.7, 0.8, 0.9$.

where

- $nsr0$ number of dies in the repeated yield loss both on a combined map and on a map by FIMER;
- $nsr1$ number of dies in the repeated yield loss only on a combined map;
- $nsr2$ number of dies in the repeated yield loss only on a map by FIMER.

B. Simulated Cases

Simulation studies deal with two kinds of gross yield loss (edge loss and center loss) with $Ysr = 0.75$, $Yr = 0.7, 0.8$, and 0.9, as shown in Figs. 9 and 10. For each Yr, 25 combined wafer maps are generated to give different random yield loss patterns. In the following section, overall simulated results will

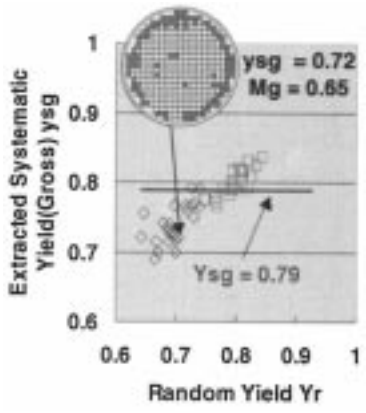

Fig. 11. Extraction of gross yield loss: Type 1 filter with fixed threshold. The wafer map shows the gross yield loss extracted by FIMER.

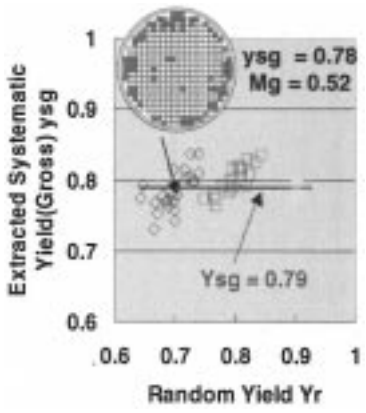

Fig. 12. Extraction of gross yield loss: Type 1 filter with adjusted threshold (threshold is adjusted for $Yr = 0.7$, 0.8, and 0.9). The wafer map shows the gross yield loss extracted by FIMER.

be discussed in relation to optimization for threshold and filter weights in the extraction of gross yield loss.

C. Optimization for Threshold

First, threshold is adjusted to minimize the extraction error of ysg for $Yr = 0.8$, and this threshold is used for $Yr = 0.7$ and $Yr = 0.9$. This is called fixed threshold, and the result is shown in Fig. 11. From the figure, it is known that threshold has to be adjusted to extract less dies for $Yr = 0.7$ and to extract more dies for $Yr = 0.9$ as gross yield loss, respectively.

Base on the result shown in Fig. 11, threshold is adjusted for each level of Yr (0.7, 0.8, 0.9) to minimize extraction error of ysg (adjusted threshold). The result is shown in Fig. 12. As shown in the figure, improvement in ysg is seen for both $Yr = 0.7$ and $Yr = 0.9$. In both fixed threshold and adjusted threshold, the die filter used for the extraction of gross yield is called the Type 1 filter.

However, when one of the extracted wafer maps for $Yr = 0.7$ is compared between the fixed threshold (Fig. 11) and the adjusted threshold (Fig. 12), the wafer map for the adjusted threshold does not look better than that for the fixed threshold.

These results are explained by the wafer maps in the Figs. 11 and 12 with the help of the histogram shown in Fig. 13.

First, in the case of the fixed threshold, from the wafer map in Fig. 11, we have the following.

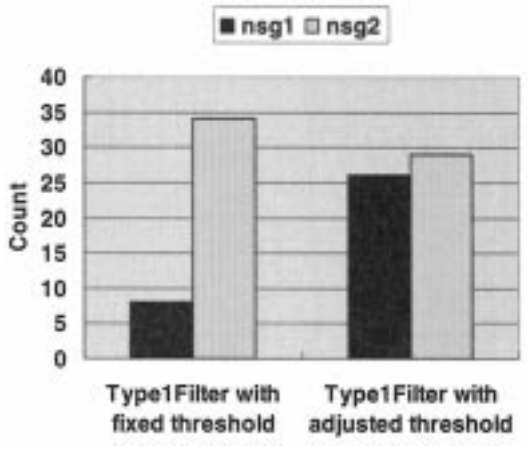

(a) (b)

Fig. 13. Histogram of $nsg1$ and $nsg2$. (a) Histogram for the wafer map in Fig. 11, fixed threshold. (b) Histogram for the wafer map in Fig. 12, adjusted threshold.

a) Most of the dies are extracted from gross yield loss region (edge) $(nsg1 \approx 0)$.
b) Additional dies are extracted from the region other than the edge $(nsg2 > 0)$

   In fact, as shown in Fig. 13, $nsg2 > nsg1$ for the fixed threshold. Therefore, as known from (10) and (11), the number of extracted dies as gross yield loss (nsg) becomes larger than the number of dies in the gross yield loss on a combined map (Nsg). As a result, $ysg < Ysg$ for $Yr = 0.7$ in the fixed threshold.

   On the contrary, in the case of the adjusted threshold, from the wafer map in Fig. 12:
c) Not enough dies are extracted from the edge $(nsg1 > 0)$.
d) Additional dies are extracted from the region other than the edge as in the case of the fixed threshold $(nsg2 > 0)$.

   And as shown in Fig. 13:
e) $nsg1 \approx nsg2$

   From e) and (10) and (11), it is known that $Nsg \approx nsg$. As a result, $ysg \approx Ysg$ for the adjusted threshold. However, as known from Fig. 13:
f) $nsg1 + nsg2$ for the fixed threshold $< nsg1 + nsg2$ for the adjusted threshold

   And from a), c), and (10),
g) $nsg0$ for the fixed threshold $> nsg0$ for the adjusted threshold

   It is known from f), g), and (12) that the adjusted threshold gives lower gross match ratio Mg than the fixed threshold as shown in Figs. 11 and 12.

D. Optimization for Filter Weights

Too-strong smoothing weakens not only noise but also signal and results in a decrease in the signal-to-noise ratio. In the case of a 3×3 filter, strength of smoothing can be adjusted by varying the center weight W_5 [14]. The effect of center weight on smoothing is shown in Fig. 14, in which a smaller center weight (stronger smoothing) weakens both noise (yield loss other than edge loss) and signal (edge loss).

To weaken the smoothing effect compared to Type 1, another filter (Type 2), which has a larger center weight than Type 1, is

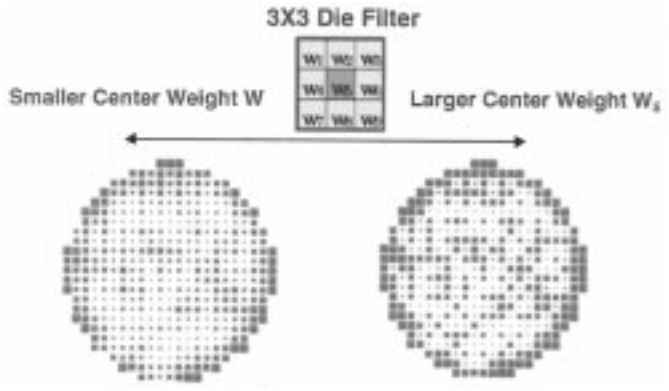

Fig. 14. Effect of center weight on smoothing: analog map (larger the square, smaller the analog value) derived in the extraction of gross yield loss for one of the wafers with edge loss in Fig. 9. Smaller center weight weakens not only the noise (yield loss other than edge loss) but also the signal (edge loss).

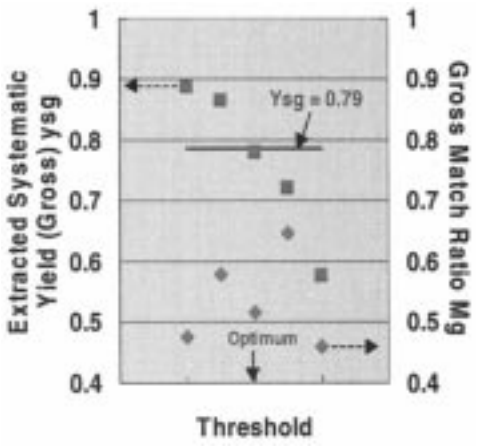

Fig. 15. Type 1 filter characteristics. An optimal threshold does not maximize Mg. One of the wafers with edge loss in Fig. 9 is used.

examined. Here, filter weights for Type 2 ($w_k^2 k = 1 \sim 9$) are given by

$$w_5^2 = C_1 w_5^1 \tag{14}$$

$$w_m^2 = C_2 w_m^1 (m = 2, 4, 6, 8) \tag{15}$$

$$w_n^2 = w_n^1 (n = 1, 3, 7, 9) \tag{16}$$

$$C_1 > C_2 > 1 \tag{17}$$

where w_5^1, w_5^2 are the center weight (see Fig. 14) for Type 1 and Type 2, respectively. In Type 2, as known from (17), filtering weight decreases as it goes away from the center.

In this study, C_2 is fixed and C_1 is adjusted to maximize Mg for the optimal threshold that minimizes the extraction error of ysg. Filter weight adjustment is explained by Figs. 15 and 16.

In Type 1, as shown in Fig. 15, the optimal threshold that minimizes the extraction error of ysg does not maximize gross match ratio Mg. On the contrary, in Type2, as shown in Fig. 16, the optimal threshold also maximizes Mg. From the figure, it is also known that Mg increases as center weight (C_1) increases until it saturates [Fig. 16(b)]. This saturation point is defined as an optimal center weight, and the filter weights with this optimal center weight are defined as optimal filter weights for Type 2.

The result for Type 2 with adjusted threshold (for each Yr) is shown in Fig. 17. From Fig. 17, it is known that Type 2 with adjusted threshold improves Mg as well as ysg compared to Type 1 with fixed threshold in Fig. 11.

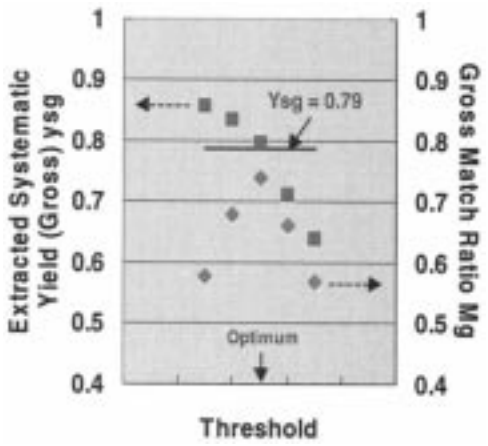

(a)

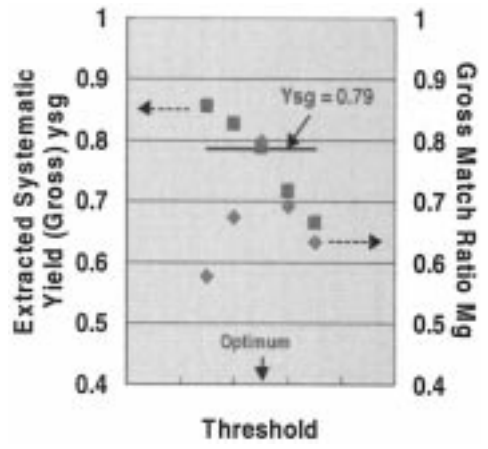

(b)

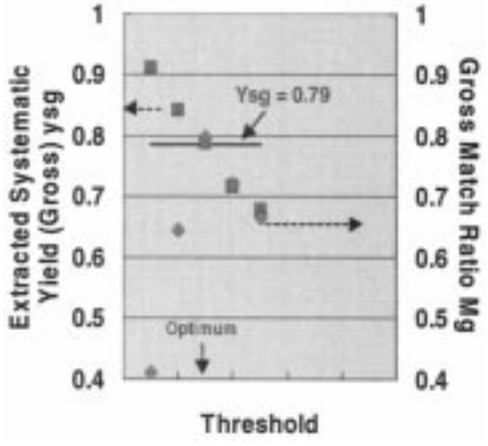

(c)

Fig. 16. Type 2 filter characteristics. An optimum threshold maximizes Mg. With the increase in center weight, Mg increases until it saturates ((b) Medium Center Weight). (a) Type 2: Small Center Weight. (b) Type 2: Medium Center Weight. (c) Type 2: Large Center Weight.

Comparisons of Mg between three types of filter/threshold for the whole wafers with edge loss in Fig. 9 and for those with center loss in Fig. 10 are shown in Fig. 18. As expected, Type 2 with adjusted threshold gives the maximum Mg for the whole wafers.

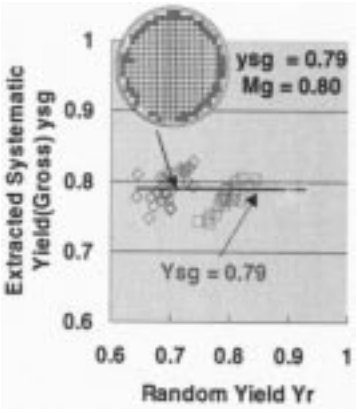

Fig. 17. Extraction of gross yield loss. Type 2 filter with adjusted threshold (threshold is adjusted for $Yr = 0.7, 0.8$, and 0.9). The wafer map shows the gross yield loss extracted by FIMER.

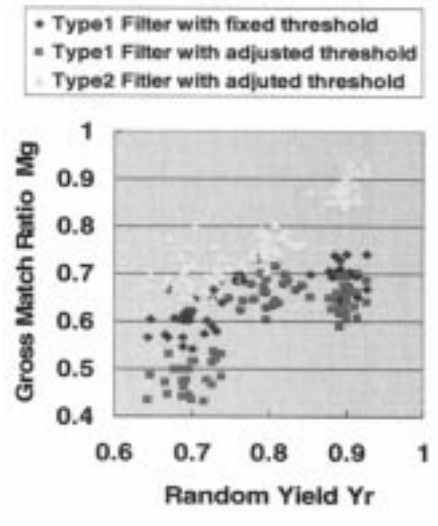

(a)

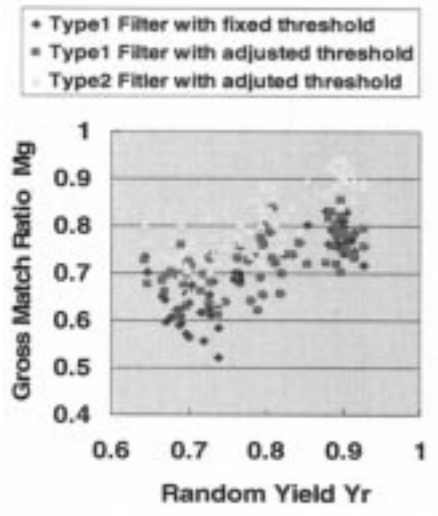

(b)

Fig. 18. Comparisons of gross match ratio Mg. (a) Edge loss case in Fig. 9 and (b) center loss case in Fig. 10.

It is also known from the figure that Mg decreases with decrease in Yr. As random yield loss increases (random yield decreases), small or medium size of clustering of failed dies occurs, as seen in the map for $Yr = 0.7$ in Figs. 9 and in 10. This clustering of failed dies is extracted as gross yield loss, as shown in the wafer maps in Figs. 11 and 12. This is considered to be the main reason for decrease in Mg.

After extracting gross yield loss, repeated yield loss is extracted by a 3×3 shot filter with fixed threshold (threshold is adjusted for $Yr = 0.8$, and the threshold is also used for $Yr = 0.7$ and 0.9). As for filter, although a simple 3×3 mean filter is used, it has been confirmed that matching ratio for repeated yield loss Mrp is high enough (0.9 or more). Optimization for filter weight for repeated loss might be needed when repeated yield loss is localized on a wafer, and will be discussed in a future paper.

The results are summarized in Fig. 19 for the edge loss case in Fig. 9 and for the center loss case in Fig. 10. As shown in the the figure, Type 2 with adjusted threshold (for the extraction of gross yield loss) gives the best results for both edge loss and center loss with an error equal to or less than 5% for three yield components.

V. Further Discussions

In FIMER, there are two kinds of parameters: threshold and a set of filter weights. In the simulation studies, threshold is adjusted to minimize extraction error of ysg for each Yr, and filter weights are adjusted to maximize gross match ratio Mg. Once filter weights are optimized, Mg can be used for threshold optimization because the threshold that maximizes Mg minimizes the extraction error of ysg, as shown in Fig. 16.

When FIMER is applied to a product wafer, a new measure to optimize threshold is to be introduced because Mg is not calculated from a probe-tested wafer. One of the procedures to apply FIMER to a product wafer is as follows.

Step 1) Optimize filter weights by simulation.
Step 2) Optimize threshold using a new measure derived from a probe-tested wafer

For a new measure in Step 2), several candidates are being investigated and will be presented in a future paper.

VI. Conclusion

In this paper, FIMER, a new method to extract three critical yield loss components (gross, repeated, and random), has been analyzed in terms of threshold and filter weights, which are the major parameters to consider. In the analysis on threshold, it has been shown that threshold has to be optimized for each level of random yield. As for filter weights, a new measure called gross match ratio is introduced for optimization. When threshold and filter weights are optimized, it has been shown that the three components are extracted with an error equal to or less than 5%. To apply FIMER to a product wafer, a new measure replacing Mg has to be introduced. Application of FIMER and further

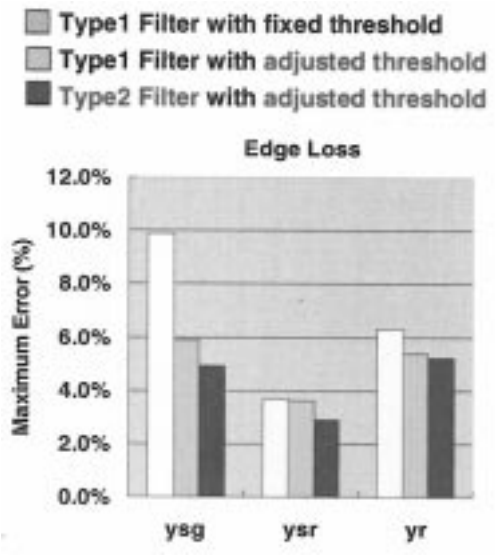

(a)

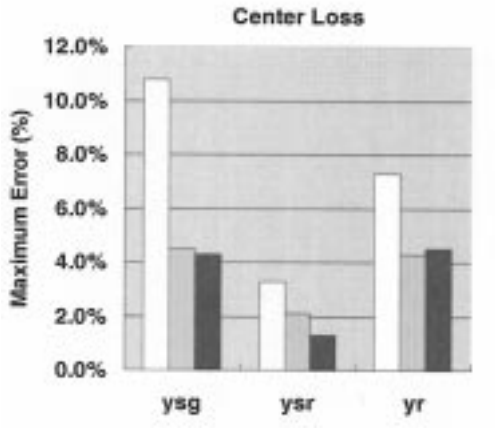

(b)

Fig. 19. Maximum error in FIMER. (a) Edge loss in Fig. 7 and (b) center loss in Fig. 8.

case studies with more variation of the size and the type of yield loss will be discussed in a future paper.

REFERENCES

[1] W. E. Ham, "Yield-area analysis: Part I—A diagnostic tool for fundamental integrated-circuit process problems," *RCA Rev.*, vol. 39, pp. 231–249, 1978.

[2] O. Paz and T. Lawson, "Modification of Poisson statistics: Modeling defects induced by diffusion," *IEEE J. Solid-State Circuits*, vol. SC-12, no. 5, pp. 540–546, 1977.

[3] R. B. Seeds, "Yield, economic, and logistic models for complex digital arrays," in *IEEE Int. Conv. Rec.*, 1967, pp. 60–61.

[4] B. T. Murphy, "Cost-size optima for monolithic integrated circuits," *Proc. IEEE*, vol. 52, pp. 1537–1545, 1964.

[5] T. Okabe, M. Nagata, and S. Shimada, "Analysis on yield of integrated circuits and a new expression for the yield," *Elect. Eng. Jpn.*, vol. 92c, no. 12, pp. 135–141, 1972.

[6] J. A. Cunningham, "The use and evaluation of yield models in integrated circuit manufacturing," *IEEE Trans. Semiconduct. Manufact.*, vol. 3, pp. 60–71, May 1990.

[7] C. H. Stapper, "Integrated circuit yield management and yield analysis: Development and implementation," *IEEE Trans. Semiconduct. Manufact.*, vol. 8, pp. 95–102, May 1995.

[8] A. Y. Wong, "A systematic approach to identify critical yield sensitive parametric parameters," in *Proc. IEEE Int. Work. Statistical Metrology*, 1997, pp. 56–61.

[9] M. Sasago, "Lithography solutions for sub-0.1 μm generations," in *Symp. VLSI Technol. Dig.*, 1998, pp. 6–9.

[10] K. Imai and T. Kaga, "A new filtering method to extract repeated defects (FIMER)," in *Proc. IEEE Int. Work. Statistical Metrology*, 1999, pp. 22–25.

[11] ——, "Highly accurate extraction of 3 critical yield loss components (gross, repeated, and random) by FIMER," in *Proc. IEEE Int. Symp. Semiconductor Manufacturing*, 1999, pp. 383–386.

[12] M. H. Hansen, D. J. Friedman, and V. N. Nair, "Monitoring wafer map data from integrated circuit fabrication process for spatially clustered defects," *Technometrics*, vol. 39, no. 3, pp. 241–253, 1997.

[13] K. Imai, "Highly accurate extraction of 3 critical yield loss components (gross, repeated, and random)—Analysis on threshold and filter weights," in *Proc. Semicon. Japan 99 STS 99*, 1999, pp. 2-58–2-64.

[14] W. K. Pratt, *Digital Image Processing*, 2nd ed. New York: Wiley, 1991.

[15] D. J. Friedman, M. H. Hansen, V. N. Nair, and D. A. James, "Model-free estimation of defect clustering in integrated circuit fabrication," *IEEE Trans. Semiconduct. Manufact.*, vol. 10, pp. 344–359, Aug. 1997.

Kiyotaka Imai (S'89–M'91) received the B.E. degree in mathematical engineering and instrumentation physics from the University of Tokyo, Tokyo, Japan, in 1982 and the M.S. degree in electrical engineering from the University of Michigan, Ann Arbor, in 1991.

From 1982–1997, he was with NKK Corporation, Kawasaki, Japan, where he engaged in device design and process development of logic products, SRAM, flash memory, and mask ROM. He also worked on the development of a measurement system using X-rays, microwave, and infrared radiation. On leave from NKK, from 1988 to 1992, he conducted research on high-speed transistors using III–V semiconductors and Si–Ge alloys at the Tokyo Institute of Technology, Tokyo, Japan, and at the University of Michigan, and also worked for the development of high-speed SRAM at Paradigm Technology Inc., San Jose, CA. In 1997, he joined KLA-Tencor Japan Ltd., where he is a Senior Project Manager in the Yield Management Consulting Group. Since 1997, he has been engaged in yield enhancement projects for both memory and logic products, working in the field of statistical yield analysis.

Toru Kaga (M'87) received the B.S. and M.S. degrees in physics and the Ph.D. degree in applied physics from Waseda University, Tokyo, Japan, in 1978, 1980, and 1989, respectively.

From 1980 to 1996, he was with tthe Central Research Laboratory, Hitachi, Ltd., Tokyo. He worked on design of nonvolatile memory devices, characterization of SiO2 and oxynitride films, design of submicrometer isolation and MOSFET's, and design and characterization for 16-Mbit to 1-Gbit DRAM processes and devices. In 1996, he joined KLA Japan Ltd., Kanagawa, Japan, where he has been working on yield-related science and yield management in ULSI manufacturing. In 1997, KLA Japan Ltd. was merged and changed its name to KLA-Tencor Japan Ltd, where he is currently a General Manager, Yield Management Consulting Group. He was a Visiting Industrial Fellow at the University of California at Berkeley from 1992 to 1993.

Dr. Kaga is a Member of the Japan Society of Applied Physics and the Institute of Electronics, Information and Communication Engineers of Japan. He was an Editorial Member of the Institute of Electronics, Information and Communication Engineers of Japan, a Committee Member of the JEIDA, and an Arrangement Chair of the International Workshop on Statistical Metrology (IWSM). He is Treasurer of IWSM and a Member of the Program Committee of the International Symposium on Semiconductor Manufacturing and the International Symposium on Microelectronic Manufacturing Technologies.